THAT Corporation

Pre-Trimmed, Very Low-Voltage
Low-Power Analog Engine® IC

THAT 4316

FEATURES

- Pre-trimmed VCA and RMS detector
- Very low supply voltage: 2.7V - 5.5V
- Low supply current: 1.2mA typ. (3.3V)
- Internal Vcc/2 divider and buffer
- Wide dynamic range: 115dB as compander

APPLICATIONS

- Companding noise reduction
  - Wireless microphones
  - Wireless instrument packs
  - Wireless in-ear monitors
- Battery operated dynamics processors
  - Compressors
  - Limiters
  - Noise Gates
  - AGCs

Description

The THAT4316 is a single-chip Analog Engine® optimized for very low-voltage, low-power operation. It incorporates a high-performance class-AB voltage-controlled amplifier (VCA) and true-RMS-responding level detector. The 16-pin QSOP part is aimed at battery-operated audio applications including companding systems for wireless microphones, wireless instruments, and in-ear monitors, as well as dynamics processors of all types. The 4316 operates from a single supply voltage down to 2.7V, drawing only 1.2mA at 3.3V.

The 4316's true-RMS-level detector improves the sound of the part over averaging or peak detectors in companding applications as well as sound mod-ifiers. This makes the 4316 ideal for many low-power dynamics processors including compressors, limiters, and gates.

The part was developed as a versatile analog engine, drawing from THAT's long history and experience with such applications. Because both VCA control ports and the RMS level detector output are independently available, the part is extremely flexible. It can be configured for a wide range of applications including single and multi-band companders with a wide range of companding ratios, plus compressors, expanders, limiters, AGCs, de-essers, and the like.

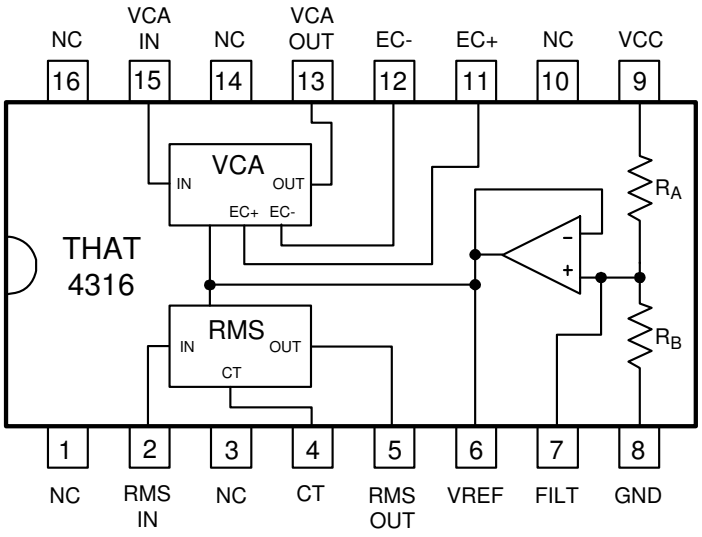

Figure 1. THAT4316 block diagram.

THAT Corporation; 45 Sumner Street; Milford, MA 01757-1656; USA
Tel: +1 508 478 9200; Fax: +1 508 478 0990; Email: info@thatcorp.com; Web: www.thatcorp.com

SPECIFICATIONS[1]

Absolute Maximum Ratings[2]

Positive Supply Voltage (V_{CC})	+6.0V	Vref Output Short-Circuit Duration	30 sec
Supply Current (I_{CC})	10 mA	Operating Temperature Range (T_{OP})	-40 to +85 ºC
I/O Pin Voltage	Supply Voltage	Junction Temperature (T_J)	-40 to +125 ºC
Ec+, Ec- to Vref Voltage	± 1V	Storage Temperature Range (T_{ST})	-40 to +125 ºC

Electrical Characteristics[3, 4]

Parameter	Symbol	Conditions	Min	Typ	Max	Units
Power Supply						
Positive Supply Voltage	V_{CC}	Referenced to GND	+2.7	3.3	+5.5	V
Supply Current	I_{CC}	No Signal				
		V_{CC}=+3.3 V	—	1.2	1.8	mA
		V_{CC}=+5 V	—	1.3	2.0	mA
Voltage Controlled Amplifier (VCA)[3]						
Max. I/O Signal Current	$i_{IN(VCA)} + i_{OUT(VCA)}$	V_{CC} = +3.3 V	—	1200	—	μA_{peak}
		V_{CC} = +5 V	—	1600	—	μA_{peak}
VCA Gain Range		E_{C+} or E_{C-} used singly	-50	—	+50	dB
Gain at 0V Control	G_0	$E_{C+} = E_{C-} = V_{REF}$	-1.5	0	+1.5	dB
Gain-Control Constant	$\Delta E_C / \Delta$Gain (dB)	-40 dB to +40 dB	—	6.1	—	mV/dB
Gain-Control Tempco	$\Delta E_C / \Delta T_{CHIP}$	Ref T_{CHIP}=27ºC	—	+0.33	—	%/ºC
Output Offset Voltage Change[4]	$\lvert\Delta V_{OFF(OUT)}\rvert$	R_2 = 4.7kΩ				
		0 dB gain	—	3	15	mV
		+15 dB gain	—	6	30	mV
Output Noise	$e_{N(OUT)}$	0 dB gain				
		22Hz~22kHz, R_1=R_2=4.7 kΩ	—	-95	-93	dBV
Total Harmonic Distortion	THD	1kHz 0dB (V_{IN} = -10dBV), $E_{C+} = E_{C-}$ = Vcc/2	—	0.03	0.15	%
Maximum VCA Control Voltage	E_{c-},E_{c+}	Ref: V_{REF}	-500	—	500	mV
VCA Control Port Input Impedance		E_{C+}, E_{C-}	400	500	600	Ω
Source Impedance at VCA Input[5]		Frequency > 320 kHz	—	—	2.5	kΩ

1. All specifications are subject to change without notice.
2. If the device is subjected to stress above the Absolute Maximum Ratings, permanent damage may result. Sustained operation at or near the Absolute Maximum Ratings conditions is not recommended. In particular, like all semiconductor devices, device reliability declines as operating temperature increases.
3. Unless otherwise noted, T_A=25ºC, V_{CC}=+3.3V.
4. See Figure 13 for component references.
4. Reference is to output offset with approximately -40 dB VCA gain.
5. Refer to the text in item 4 of the 4316 and 2182 comparison on page 6.

Electrical Characteristics (con't)[3]

Parameter	Symbol	Conditions	Min	Typ	Max	Units
RMS Level Detector						
RMS reference input current	i_{in0}		—	7.2	—	μA_{rms}
Output Voltage at Reference i_{IN}	$e_{O(0)}$	$i_{IN} = i_{in0}$ = 7.2 µA RMS, Ref:V_{REF}	-13	0	+13	mV
Output Error at Input Extremes	$e_{O(RMS)error}$	i_{IN} = 200 nA RMS	-3	±1	3	dB
		i_{IN} = 150 µA RMS	-3	±1	3	dB
Output scale factor	$\Delta e_{O(RMS)}/\Delta i_{in}$ (dB)	0.72 µA< $i_{IN(RMS)}$ < 72 µ A	—	6.1	—	mV/dB
Scale Factor Match to VCA		-20 dB < VCA gain < +20 dB				
		0.72 µA< $i_{IN(RMS)}$ < 72 µ A	0.92	1	1.08	
Rectifier Balance		$I_{in} = \pm I_{in0}$ DC_{IN}	-1	0	+1	dB
Timing Current	I_T		—	7.2	—	µA
Filtering Time Constant	τ	T_{CHIP} = 27 ºC		3611 X C_T		s
Output Tempco	$\Delta e_{O(RMS)}/\Delta T_{CHIP}$	Ref T_{CHIP} = 27 ºC	—	+0.33	—	%/ºC
Load Resistance	R_L	-400mV < V_{OUTRMS}< +230mV, Ref:V_{REF}	400	—	—	Ω
Capacitive Load	C_L		—	—	100	pF
Vcc/2 Reference Generator[3]						
V_{REF} Output Current	$I_{OUT(VREF)}$		-1.25	—	+1.25	mA
V_{REF} Load Capacitance	$C_{L(VREF)}$		—	—	100	pF
V_{REF} Output Voltage	V_{REF}	No load on V_{REF}	Vcc/2-12	Vcc/2	Vcc/2+12	mV
Voltage Divider Resistors	R_A, R_B		—	48	—	kΩ
Performance as a Compander (through an encode-decode cycle)						
Dynamic Range	(max signal level)-(no signal A-weighted output noise)		—	115	—	dB
Distortion	THD	f = 1 kHz	—	0.15	—	%
Frequency response	-20 dB re: Max Signal	20 Hz ~ 20 kHz	—	± 1.5	—	dB

REPRESENTATIVE DATA[6,7]

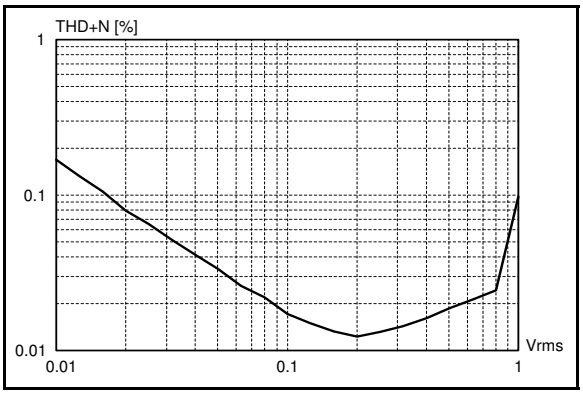

Figure 2. VCA THD+N vs. Level at 0 dB gain[8].

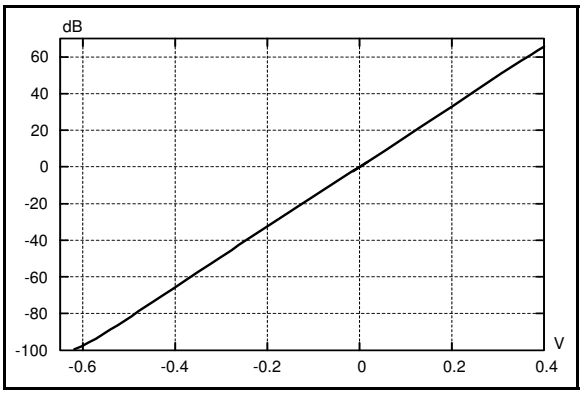

Figure 6. VCA Gain vs. Control Voltage (V_{Ec+}-V_{Ec-}).

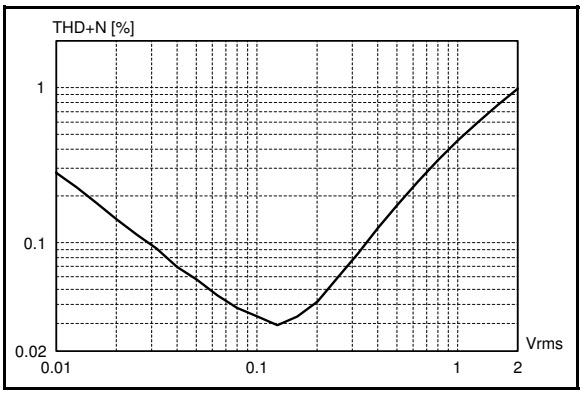

Figure 3. VCA THD+N vs. Input Level at -15 dB gain[8].

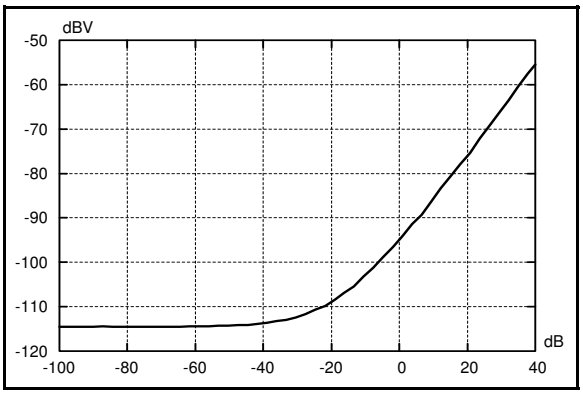

Figure 7. VCA Noise vs. Gain[8].

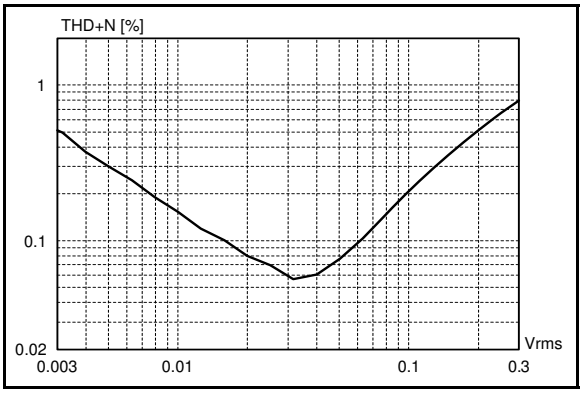

Figure 4. VCA THD+N vs. Input Level at +15 dB gain[8].

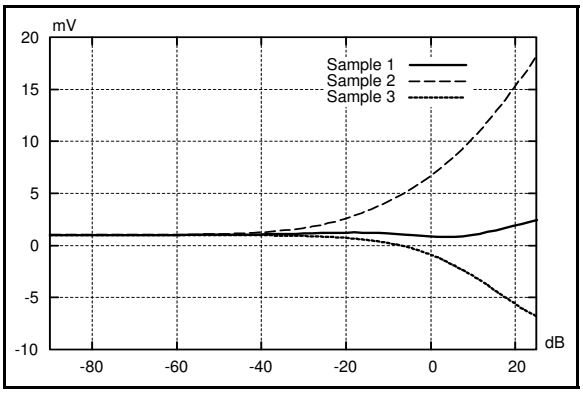

Figure 8. VCA Offset (at VCA Out in Fig. 13) vs. Gain.

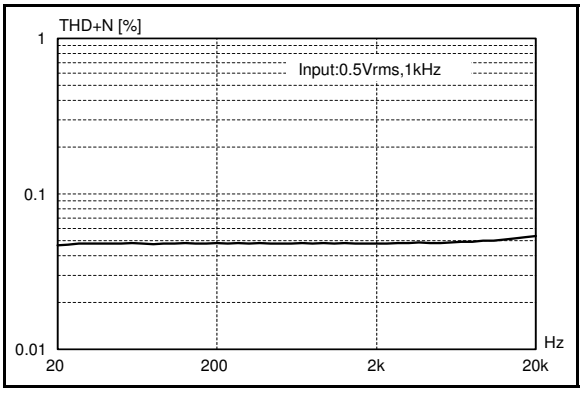

Figure 5. VCA THD+N vs. Frequency at 0dB gain[9].

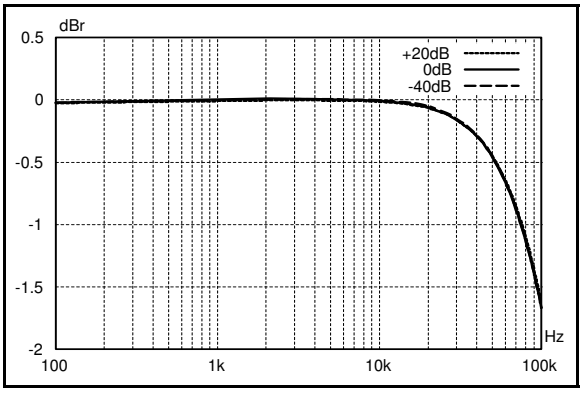

Figure 9. VCA Frequency Response for various Gains[10].

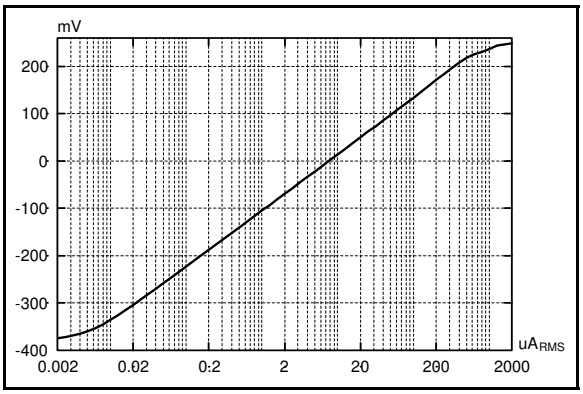

Figure 10. RMS Output vs. Input Current i_{IN}.

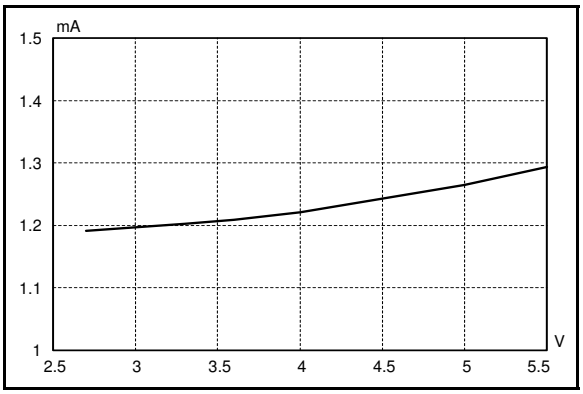

Figure 12. Supply Current vs. Supply Voltage.

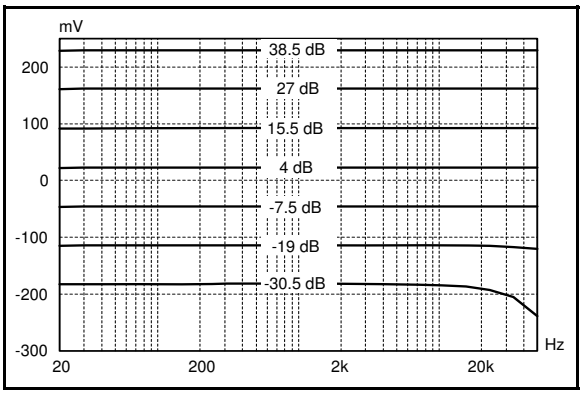

Figure 11. RMS Frequency Response vs. Level [9].

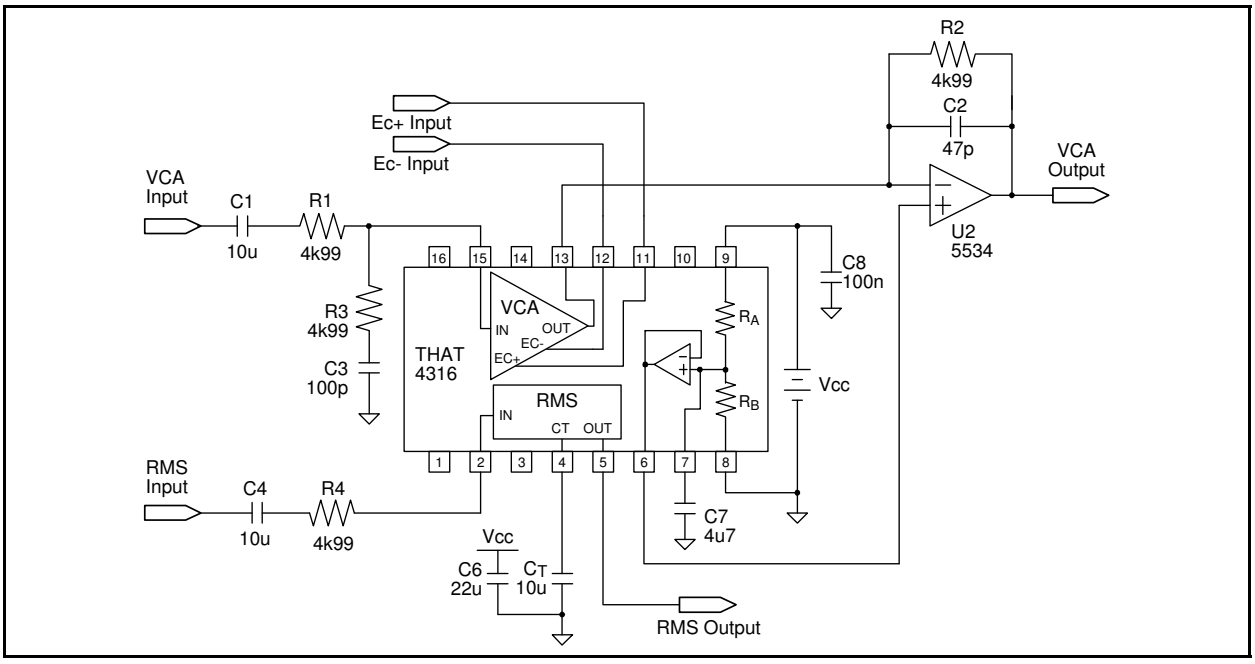

Figure 13. The 4316 VCA and RMS detector test circuit.

6. Unless otherwise noted, T_A=25ºC, V_{CC}=+3.3V, f=1kHz
7. The test circuit is shown in Figure 13.
8. Measured with an Audio Precision System One with 22 kHz bandwidth.
9. Measured with an Audio Precision System One with 80 kHz bandwidth.
10. Measured with an Audio Precision System One with >500 kHz bandwidth.

Theory of Operation

The THAT 4316 Analog Engine combines an exponentially controlled Voltage-Controlled Amplifier (VCA) with a true-RMS-responding level detector to produce a versatile dynamics processor. The part is implemented in a low-voltage Bi-CMOS process. It delivers wide bandwidth and excellent audio performance while consuming less than 4mW when running from 3.3V.

For details of the theory of operation of the VCA and RMS Detector building blocks, we refer interested readers to THAT Corporation's data sheets on the 2180-Series VCAs and the 2252 RMS Level Detector.

The VCA — in Brief

The VCA in THAT 4316 is based on THAT Corporation's highly successful complementary log-antilog gain cell topology — The Blackmer™ VCA — as used in THAT 2180-Series IC VCAs. We modified the traditional design so that the VCA works in a power-efficient class-AB mode under supply voltages as low as 2.7V using a Bi-CMOS process. The VCA symmetry is trimmed during wafer probe for minimum distortion. No external adjustment is allowed.

Input signals are currents in the VCA IN pin (pin 15). This pin is a virtual ground with dc level approximately equal to V_{REF}; in normal operation, an input voltage is converted to a current via an appropriately sized resistor. Referencing Figure 13, the VCA input voltage is converted to a current based on the value of R_1. Because any current associated with dc offsets present at the input pin (for instance, any dc offset from V_{REF} in the preceding stages) will be modulated by gain changes (thereby becoming audible as thumps), the input pin is normally ac-coupled (C_1).

The VCA output signal (at pin 13) is also a current, in phase with respect to the input current. In normal applications, the output current is converted to a voltage via an external op-amp (U2 in Figure 13), where the ratio of the conversion is determined by the feedback resistor R_2 connected between U2's output and its inverting input. **The signal path through the VCA and op-amp (from "VCA Input" to "VCA Output" in Figure 13) is inverting. Note that this is in contrast to other THAT Corporation ICs featuring a Blackmer™ VCA (e.g., THAT 4315 or 2180 series), which have a non-inverting signal path.**

The gain of the VCA is controlled by the voltage applied between E_{C+} (pin 11) and E_{C-} (pin 12). Note that any unused control port should be connected to V_{REF}. The gain (in decibels) is proportional to (V_{EC+} – V_{EC-}) (see Figure 6). The constant of proportionality is typically 6.1mV/dB. Note the limits to the control voltages at E_{C+} and E_{C-} in the specifications section.

The VCA's noise performance varies with gain in a predictable way as shown in Figure 7. At large attenuation (<-50dB), the noise floor is limited to about -114dBV by the input noise of the output op-amp U2 (a 5534 type) and its feedback resistor. At 0dB gain, the noise floor is ~ -95 dBV as specified. In the vicinity of 0dB gain, the noise increases almost linearly with the gain. This applies to the whole positive gain region. As gain drops below -20dB, the noise floor decreases more slowly than the gain and tends to saturate below -40dB.

While the 4316's VCA circuitry behaves similarly to that of the THAT 2180-Series, there are several important differences, as follows:

1. At +3.3 V V_{CC}, approximately 1.2 mA is available from the 4316 for the sum of VCA input and output signal currents. This increases to ~1.6mA at +5V V_{CC}.

2. A SYM control port (similar to that on the 2180 VCA) exists, but is driven from an internally trimmed current generator. This current flows into either the positive or negative control port, depending on the (internal) trimming direction, and must be supplied by whatever circuitry drives this port.

3. Each of the 4316 VCA control ports is connected to an internal 2:1 resistive voltage divider (internally terminating at V_{REF}). These scale the VCA gain control constant from the internal ~3mV/dB to match the RMS detector output characteristic. The control port input impedance is 500Ω ±100Ω, so the driving circuitry must be capable of supplying the required current into this load.

4. To maintain stability over the wide range of possible VCA gains, the 4316 VCA's internal CMOS transconductance amplifier requires that the source impedance at the VCA input pin must be kept under 2.5kΩ above 320kHz. R_3 and C_3 in Figure 13 are provided to accomplish this. See the Applications section for more ideas on how best to address this issue.

The RMS Detector — in Brief

The 4316's detector computes RMS level by rectifying the input current signals, converting the rectified current to a logarithmic voltage, and applying that voltage to an internal log-domain filter. The output signal is a dc voltage proportional to the decibel-level of the RMS value of the input signal current. Some ac component (at twice the input frequency, $2f_{in}$) remains superimposed on the dc output. The ac signal is attenuated by the internal log-domain filter, which constitutes a single-pole rolloff with cutoff determined by an external capacitor.

As in the VCA, the detector's input signals are currents to the RMS IN pin (pin 2). This pin is a virtual ground with dc level equal to V_{REF}, so a resistor is normally used to convert input voltages to the desired current. The level detector is capable of accurately resolving signals well below 100nA (see Figure 10). However, if the detector is to accurately track such low-level signals, ac coupling is required.

Note also that small, low-voltage electrolytic capacitors used for this purpose may create significant leakage if they support half the supply voltage, as is the case when the source is dc-referenced to ground. To ensure good detector tracking to low levels, the input coupling capacitor's leakage (given the voltage across it in the application) should be insignificant compared to the lowest signal current to be resolved.

The internal log-domain filter cutoff frequency is usually placed well below the frequency range of interest. For an audio-band detector, a typical value would be 5Hz, or a 32ms time constant. The filter's time constant is determined by an external timing capacitor, C_T, attached to the CT pin (pin 4), and an internal current source (I_T) connected between GND and the CT pin. This current source is fixed at ~7.2μA with a tolerance of ~±20%. The resulting time constant in seconds is approximately equal to 3611 times the value of C_T (in farads). Note that, as a result of the mathematics of RMS detection, the attack and release time constants are fixed in their relationship to each other.

The RMS detector is capable of driving large spikes of current into C_T when the audio signal at the RMS detector's input increases suddenly. This current is drawn from V_{CC} (pin 9), fed into C_T at pin 4, and returns to the power supply through the ground end of C_T. If not handled properly through layout and bypassing, these currents can mix with the audio, producing unpredictable and undesirable results. As shown in Figure 13, a local bypassing capacitor, like C_6, from the V_{CC} pin to the ground end of the timing capacitor C_T, is strongly recommended to keep these currents out of the ground structure of the circuit.

The dc output of the detector is scaled with the same constant of proportionality as the VCA gain control, ~6.1mV/dB. The detector's 0dB reference current (i_{in0}, the RMS input current which causes the detector's output to equal V_{REF}), is approximately equal to 7.2μA, the same value as I_T. The RMS detector output stage is capable of directly driving either of the 500Ω VCA control ports to the limits of the detector output voltage. It is also capable of driving up to 100pF of capacitance.

Frequency response of the detector (see Figure 11) extends across the audio band for a wide range of input signal levels. Note, however, that it does fall off at high frequencies at low signal levels.

Differences between the 4316's RMS level detector and that of the THAT 2252 include the following:

1. The rectifier in the 4316 RMS detector is internally balanced by design, and cannot be adjusted externally. The residual mismatch in the 4316 will not significantly increase ripple-induced distortions in dynamics processors over that caused by the signal ripple alone.

2. The time constant of the 4316's RMS detector is determined by the combination of the external timing capacitor and the internal current source, I_T. A resistor is not normally connected directly to the CT pin on the 4316.

3. The 0dB reference input current, or level match, is equal to approximately I_T. However, as in the 2252, the level match will be affected by any additional currents drawn from the CT pin.

Reference Voltage

The 4316 input and output signals, as well as the VCA control voltages, must be biased to a reference voltage between V_{CC} and ground. For optimal performance, the reference must have low AC impedance and noise. The 4316 contains an internal voltage divider (RA, RB) and buffer amplifier (OA1) for this function, as shown in Figure 14.

Capacitor C_7 is required from the FILT pin (pin 7) to ground. It serves to minimize the influence of the thermal noise of the resistive divider on the rest of the circuity, as well as to filter out any supply-related noise. A 4.7μF capacitor results in a lowpass pole of ~1.4Hz with the internal divider impedance of 24kΩ. This is sufficient for most applications. Larger values provide additional filtering at the expense of longer settling times after power is applied.

The FILT pin is internally connected to the input of unity gain buffer OA1. The output of OA1 is available at the VREF pin (pin 6). The buffer also drives the requisite internal nodes, including one end of each of the control-port voltage dividers. Because most of OA1's output current is required to drive the low-impedance dividers at the VCA control ports, designers should take care not to draw too much current externally from this pin. Limit the external current to within +/-1.25mA.

Pins 1, 3, 14 and 16, are not connected internally; we suggest they be connected to VREF in a PCB layout so that they provide shielding to the VCA and RMS input pins.

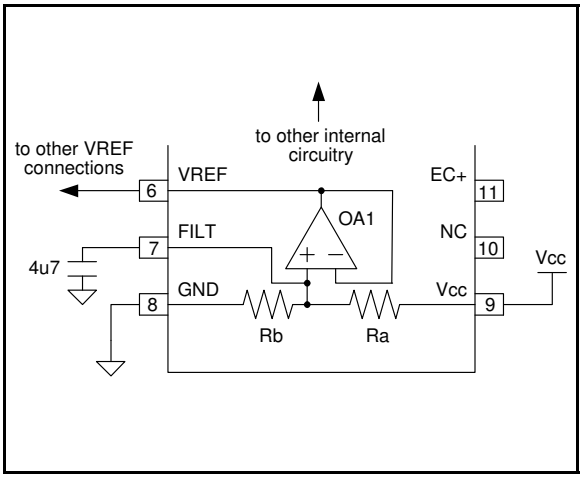

Figure 14. Internal voltage reference generator.

Applications

The 4316 provides the basic building blocks for a wide variety of dynamics processing applications: an exponentially controlled VCA and a logarithmic RMS detector. These elements are especially versatile because the audio performance of designs using these blocks is determined primarily by the control loop (or "side chain") from the detector to the VCA control port. Theory of the interconnection of exponentially controlled VCAs and log-responding level detectors is covered in THAT Corporation's design note DN01A, "*The Mathematics of Log-Based Dynamic Processors*".

Perhaps the most important application for the 4316 is wireless audio companding systems. In this data sheet, we cover this application in some detail. However, many other configurations are possible, including all those covered within THAT's collection of application notes for dynamics processors (though shown with previous VCA/detector parts or Analog Engines). For assistance with these and any other applications, please contact our applications engineers at apps_support@thatcorp.com.

Noise Reduction (Compander) Configurations

A primary use of the 4316 is for noise reduction systems, particularly within battery-operated devices. In these applications, one 4316 is configured for use as a compressor (or encoder) to condition audio signals before feeding them into a noisy channel such as a radio-frequency (RF) link. A second 4316, configured as an expander (or decoder), is located at the receiver end of the noisy channel.

The compressor reduces the dynamic range of the audio signals so that it can fit better through a channel with limited dynamic range. The expander works in an opposite, complementary fashion to restore the dynamic range of the original audio signal (as present at the input of the compressor).

As shown in Figure 17, during low-level audio passages, the compressor increases signal levels, bringing them up above the noise floor of the channel. At the receiving end, the expander reduces the signal back to its original level, in the process attenuating the channel noise.

During high-level audio passages, the compressor decreases signal levels, reducing them to fit within the headroom limits of the channel. The expander then increases the signal back to its original level. While the channel noise may be increased by this action, in a well-designed compander, the noise floor will be masked by the high-level audio signal.

Advantages of True-RMS-Level Detection

The 4316's RMS detector has the property that it responds faster to large increases in signal level than to small ones. This is because it responds to the square of the input signal, instead of the signal itself. Essentially, its attack time varies, becoming shorter for large level changes than that for small ones. This mimics the behavior of the human ear, resulting in more "musical" response to audio signals than for average or peak responding detectors.

In companding applications, the "variable" attack time ensures that overloads are kept short in duration, because the compressor responds quickly in cases where a low-level audio signal (causing high VCA gain) is followed suddenly by a much higher level signal (which reduces the VCA gain over time as the detector acquires the new level). This minimizes the duration of overloads for a given time constant when compared to those using average responding detectors.

Another advantage of RMS detection over average or peak detection is that it is relatively insensitive to phase shifts in the signal being measured. This is particularly helpful in companding applications because low- and high-frequency phase shifts common in a bandlimited transmission channel cause less difference between the compressor's detector reading and that of the expander. This ensures better tracking between the expander and detector in real-world applications.

The combination of insensitivity to phase shift and variable attack behavior causes companders based on true-RMS detection to sound better than those based on either average- or peak-responding detectors.

Versatility in Compander Design

The 4316 was designed to facilitate the design of a wide variety of companding noise reduction systems. The RMS detector responds accurately over a wide range of input current (Figure 10), while the VCA responds accurately to a wide range of gain commands (Figure 6). The RMS output and the VCA control inputs are fully configurable, which makes it easy to configure the 4316 for companding ratios different from the traditional 2:1. (See the section "3:1 Compander" below for one such example.)

The 4316 supports a wide range of compander designs (and more), including simple 2:1 wide range (level-independent) systems, level-dependent systems with thresholds and varying companding slopes, systems including noise gating and/or limiting, and systems with varying degrees of pre-emphasis and filtering in both the signal and control paths. Generally, these variations can be accomplished by conditioning the detector side chain rather than the audio signal itself. The audio signal passes through as little as two VCAs and two opamps, and still supports multiple ratios, thresholds, and time constants.

In this datasheet, we show the part used in three example designs. First is a simple 2:1 companding noise reduction system. Next, we show a high-performance 2:1 compander with pre- and

de-emphasis networks in the signal path and pre-emphasis in the detector path. Finally, we present a 3:1 compander with pre- and de- emphasis in the signal path and pre-emphasis in the detector path.

One other minor point is that companders designed using the 4316 are generally compatible with those using other THAT Analog Engine and discrete VCA or RMS detector ICs. For example, a 4316 may be configured as a low-voltage, low-power-consumption compressor for the battery-powered transmitter in a wireless microphone or instrument belt pack, and paired with a higher-voltage, higher-power-consumption 4301 or 4305 as the complementary expander in the companion AC-powered receiver.

Simple Compander Design

Basic 2:1 Encoder

The encoder in a wireless companding system is generally a feedback compressor located in the transmitter, operating from a battery supply. Figure 15 shows a basic 2:1 encoder. The blocks within the bold outline are the three functional circuits in the 4316, *i.e.*, a VCA, an RMS detector and a reference generator. Following the mathematical simplifications taught in DN01A, the steady-state transfer function of this circuit is :

$$OUT_C = \frac{1}{(K_C+1)}(IN_C + G_C + K_C \cdot RMS_{0C}) \quad (1)$$

where,

$$OUT_C = 20\log_{10}(V_{outC}), \quad (2)$$

$$IN_C = 20\log_{10}(V_{inC}), \quad (3)$$

$$G_C = 20\log_{10}\left(\frac{R_2}{R_1}\right), \text{ and} \quad (4)$$

$$RMS_{0C} = 20\log_{10}(V_{0C}). \quad (5)$$

IN_C and OUT_C are the compressor's voltage input V_{inC} and output V_{outC} in dBV, respectively. G_C is the compressor's signal path gain in dB; in Figure 15, G_C is determined by the ratio of R_2 to R_1 as in Equation 4 and is 0dB. K_C is the linear gain (in V/V) between the compressor RMS detector output and VCA control port. (K_C is 1 in Figure 15 since the detector output is connected directly to the VCA E_{C-} port.) Finally, RMS_{0C} is the dBV value of the detector reference voltage, V_{0C}, which causes i_{in0} (the RMS input reference current), to flow in the compressor detector's input.

$$V_{0c} = i_{in0}R_3, \quad (6)$$

where R_3 is the detector's input resistance (4.99kΩ) in Figure 15. Hence, V_{0C} is 35.9mVrms and RMS_{0C} is -28.9dBV. For this example, the compressor output OUT_C is always half of IN_C plus a fixed offset of $(G_C+RMS_{0C})/2$, yielding a compression ratio of 2:1. The compression ratio (CR), is generally defined in Equation 7:

$$CR = K_C + 1. \quad (7)$$

At the 4316 VCA input, R_4 (4.99kΩ) and C_5 (100pF) comprise the compensation network required to keep the VCA's internal amplifier stable for all gains. (C_2 performs a similar function for U2, neutralizing the VCA's output capacitance plus any stray layout capacitance appearing at the inverting input of U2.)

The RMS detector output is tied directly to the VCA's negative control port, E_{C-}. (This is what makes

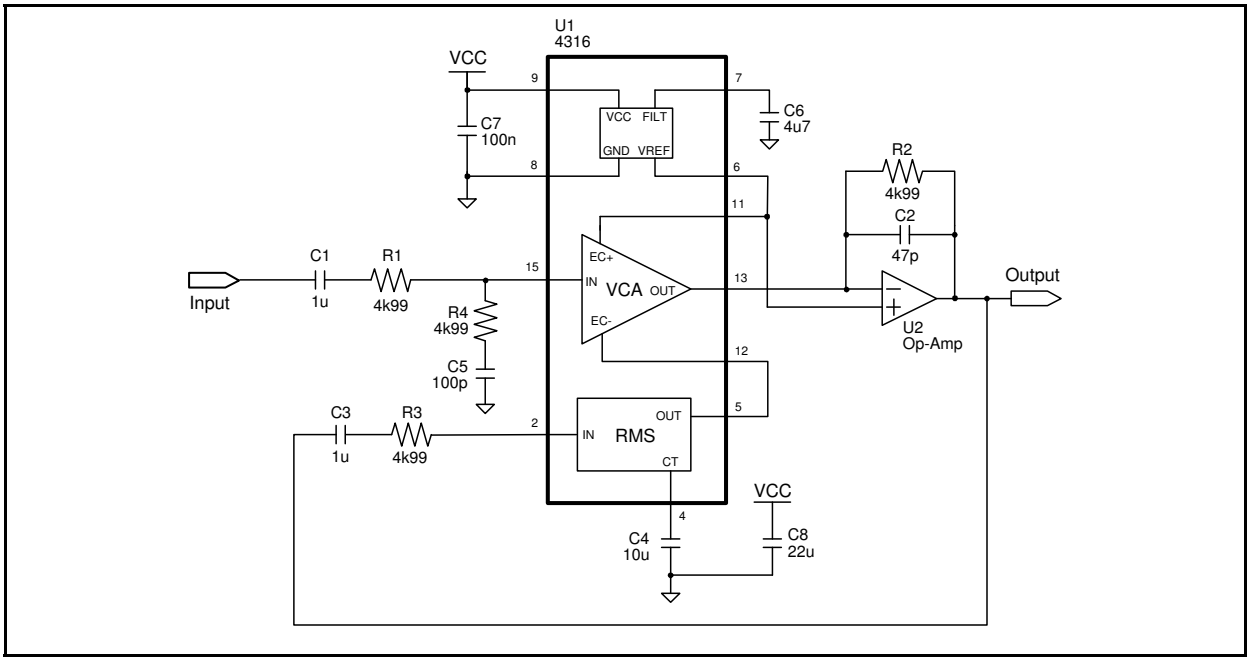

Figure 15. Basic 2:1 Compressor using 4316.

K_C=1, and sets CR at 2:1.) Because the RMS output connects to the negative-sense control port, E_{C-}, this circuit acts as a compressor. C_4 (10μF) sets the RMS detector time constant to approximately 36msec.

As described in the Theory of Operation section "The RMS Detector - In Brief", the RMS detector is capable of driving large spikes of current into C_4 in Figure 15. To prevent these currents from upsetting circuit grounds, V_{CC} should be bypassed to a point very near the grounded end of C_4 with a capacitor equal to or greater than the value of C_4. 22μF C_8 in Figure 15 serves this purpose. The grounded ends of these two capacitors should be connected together before being tied to the rest of the ground system. This will ensure that the current spikes flow within the local loop consisting of the two capacitors, and stay out of the ground system. This requirement applies to the decoder and other applications of the THAT4316 as well.

Basic 2:1 Decoder

Figure 16 shows the THAT4316 configured as a 2:1 decoder. This is a feedforward expander intended to complement the encoder of Figure 15. It is optimized for low-voltage operation, as might be the case for a decoder in an in-ear monitoring system which runs from a battery power. The expander steady-state transfer function is:

$$OUT_E = (K_E + 1)IN_E + G_E - K_E \cdot RMS_{0E}, \quad (8)$$

where

$$OUT_E = 20\log_{10}(V_{outE}), \quad (9)$$

$$IN_E = 20\log_{10}(V_{inE}), \quad (10)$$

$$G_E = 20\log_{10}\left(\frac{R_{11}}{R_{10}}\right), \text{ and} \quad (11)$$

$$RMS_{0E} = 20\log_{10}(V_{0E}). \quad (12)$$

As in Equation 1, IN_E and OUT_E are the dBV values of the expander's voltage input V_{inE} and output V_{outE}, respectively. G_E is the expander signal path gain in dB, which is 0 dB here as well. K_E is the gain in linear terms (V/V) between the expander detector output and VCA control port; it is unity here. RMS_{0E} is the dBV value of the expander detector's reference voltage V_{0E}, which is calculated using Equation 6 with the input resistor R_{12} (4.99kΩ). As in the encoder, it is also -28.9dBV.

Because, in Figure 16, the detector's output is connected directly to the VCA positive control input, the expander's output OUT_E will always double its input IN_E, except for a fixed offset (G_E-RMS_{0E}). The expansion ratio is thus 2:1, and given generally by Equation 13:

$$ER = K_E + 1. \quad (13)$$

Since the 4316 VCA is not stable unless it sees a source impedance of 2.5kΩ or less at high frequencies, another compensation network (R_{13} & C_{14}) is provided to maintain stability. 47pF C_{11} maintains stability in U2, just as C_2 does Figure 15.

In this instance, the RMS detector output is connected to E_{C+}; this reverses the polarity of the control signal relative to the encoder, and makes this circuit an expander rather than a compressor.

System Performance

The encoder and decoder in Figure 15 and 16 form a compander system. To a first approximation,

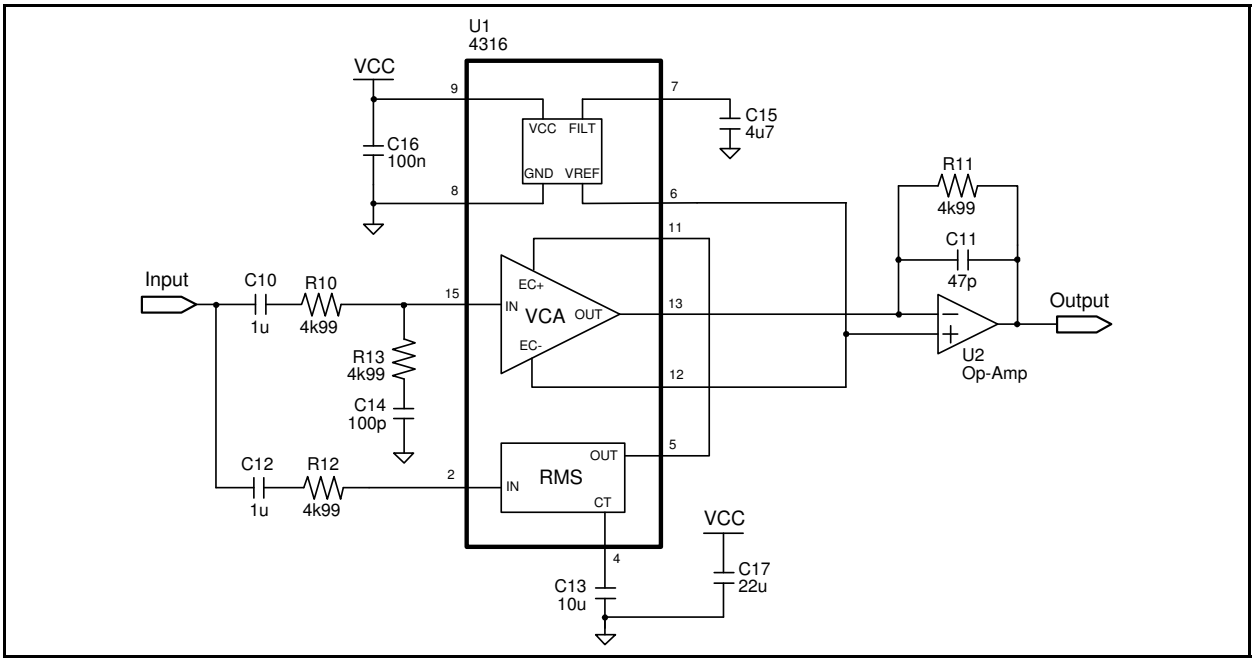

Figure 16. Basic 2:1 Expander using 4316.

the output of Figure 15 will be connected to the input of the Figure 16 expander. (The two are usually connected by an RF link, which should be relatively transparent within the audio band, except for noise.)

Static Performance

Assuming that both VCA and RMS detectors match well, as the detectors have identical input resistor values, the reference voltage terms, i.e., $K_C \bullet RMS_{0C}$ and $K_E \bullet RMS_{0E}$, in Equations 1 and 8 cancel each other. So the overall compander system transfer function becomes:

$$OUT_E = IN_C + G_C + G_E \quad (14)$$

With zero dB gain in both the encoder and decoder, the compressor input is fully recovered at the expander output. The behavior of this companding system is shown in Table 1. The columns labeled Encoder Out and Decoder Out use the previous equations to generate signal and gain values. The Encoder VCA Gain is the difference between Encoder Out and Encoder In; The Decoder VCA Gain is calculated similarly using Decoder Out and Decoder In. These two gains have the same absolute value but opposite polarity. The values in the column labeled i_{in_RMS}, which is the detector's RMS input current, are derived using the equation:

$$i_{in\_RMS} = \frac{10^{\frac{EncoderOut}{20}}}{R_{in\_RMS}}, \quad (15)$$

where R_{in_RMS} is the detector input resistance (4.99kΩ in Figure 15 and 16).

Figure 17 presents this data in the form of a "butterfly diagram" for the 2:1 compander. Signal levels are shown from the encoder input, through its output, to the decoder output. The encoder compresses its input dynamic range by a factor of 2, its CR, while the decoder reverses the process and restores the signal back to its original at the decoder output. Hence, only half of the signal dynamic range is required for the transmission channel between the encoder and decoder.

The encoder VCA gain varies from -14dB to +36dB, which covers half of the input dynamic range as well, while the decoder VCA's gain varies from -36dB to +14dB. Both these ranges easily fit within the capabilities of the 4316 VCA. The RMS input current range is also easily accommodated.

Dynamic Performance

While the VCA gains in both the compressor and expander change with signal levels, of course the changes are not instantaneous. As noted earlier, the RMS detector used in THAT's Analog Engines, including the 4316, behaves favorably when faced with changing signal levels. Its quick response to sudden overloads ensures that the compressor reacts appropriately to minimize transient overloads in the compressor and the subsequent channel. And, its insensitivity to phase changes in the signal means

Encoder In	Encoder VCA Gain	Encoder Out/ Decoder In	i_{in_RMS}	Decoder VCA Gain	Decoder Out
(dBV)	(In dB)	(dBV)	(µA)	(In dB)	(dBV)
0	-14	-14	38.00	14	0
-10	-9	-19	21.40	9	-10
-20	-4	-24	12.00	4	-20
-30	1	-29	6.75	-1	-30
-40	6	-34	3.80	-6	-40
-50	11	-39	2.14	-11	-50
-60	16	-44	1.20	-16	-60
-70	21	-49	0.676	-21	-70
-80	26	-54	0.380	-26	-80
-90	31	-59	0.214	-31	-90
-100	36	-64	0.120	-36	-100

Table 1. 2:1 compander transfer characteristics.

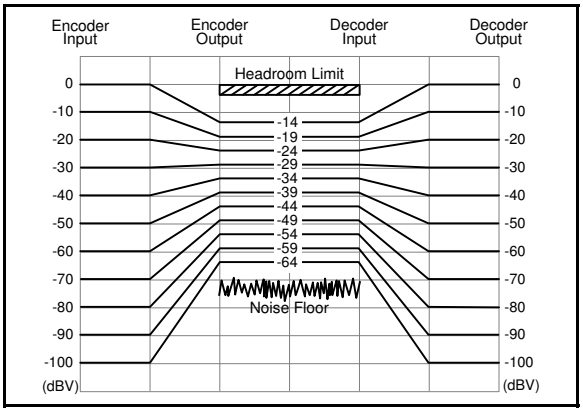

Figure 17. 2:1 compander butterfly diagram.

that the expander and compressor detectors will deliver consistently similar level readings despite the band-limiting in the transmission channel.

Nonetheless, to ensure good dynamic tracking, the time constants of both the compressor and expander RMS detectors must be the same. The time constants are controlled by the internal timing current I_T, and the external timing capacitor (C_4 and C_{13} in the two schematics). The internal timing current is controlled to within ~±20% of its nominal value. This tolerance adds to that of the timing capacitors. For the best possible tracking, THAT recommends using tight-tolerance capacitors.

Another consideration is distortion. At low frequencies, the compressor RMS detector output contains significant ripple at twice of the input frequency ($2f_{in}$). The amount of this ripple increases as frequency decreases. The ripple adds a time-varying component to the steady-state VCA gain. The ripple amplitude modulates the signal in the VCA, resulting in third harmonic distortion ($3f_{in}$) in the output of the compressor. This amounts to a "squashing" of the tops and bottoms of the input sine wave, since the detector output is the highest during those portions of the input signal.

The expander RMS detector output generally contains the same ($2f_{in}$) ripple in the same phase relationship to the fundamental as that of the compressor. And, if the distortion components (at $3f_{in}$)

are not phase-shifted with respect to the fundamental (f_{in}), then the ripple in the expander RMS detector output will reverse the dynamic effect of that in the compressor, and the distortion in the compressor output will be reduced or even canceled in the expander output. But, to make this work, the low-frequency phase shift of the channel must be very small indeed. System designers should bear this in mind if low distortion is important at low frequencies.

High-Performance 2:1 Compander

While the compander in Figure 15 and Figure 16 performs adequately in some applications, a few minor changes can result in substantially improved overall performance. The following compander implementation adds pre- and de- emphasis to the signal path and pre-emphasis to the detector path. Pre-emphasis in the encoder signal path helps overcome the "acqua noise" characteristic of the FM RF channel by raising the level of higher frequency portions of the signal while it is in the transmission channel. The de-emphasis in the decoder brings the frequency response of the signal back to flat while simultaneously lowering the noise floor of the channel. The pre-emphasis in the detector paths alleviates high-frequency overload due to the signal path pre-emphasis.

High-Performance 2:1 Encoder

The encoder shown in Figure 18 implements pre-emphasis in the signal path by means of a non-inverting stage with op-amp U3, R_6, R_7, and C_{10}. Equation 1 from the basic encoder discussion is still valid, but both the signal path gain G_C and the detector reference level RMS_{OC} become frequency dependent due to the associated pre-emphasis networks. G_C is expressed in the equation below,

$$G_C = 20\log_{10}\left(\frac{R_2}{R_1}\frac{sC_{10}(R_6+R_7)+1}{sC_{10}R_6+1}\right). \quad (16)$$

The 2nd term inside the log is introduced by the signal-path pre-emphasis network. Its bode plot is shown in Figure 19. The gain (in dB) shown is the ratio of the signal at the output of U3 to its non-inverting input. The zero frequency f_1 and pole frequency f_2 are calculated using the equations:

$$f_1 = \frac{1}{2\pi(R_6+R_7)C_{10}}, \quad (17)$$

$$f_2 = \frac{1}{2\pi R_6 C_{10}}. \quad (18)$$

At frequencies well below f_1 (391Hz), the gain is 0dB due to the effect of C_{10}. As frequency increases beyond f_1, the gain starts to increase at 6dB/octave, then flattens out at f_2 (2.34kHz).

So, the low-frequency ($<<f_1$) compressor gain G_{C_LF} is:

$$G_{C\_LF} = 20\log 20_{10}\left(\frac{R_2}{R_1}\right) \cong 10\text{dB}, \quad (19)$$

while the high-frequency ($>>f_2$) gain, G_{C_HF}, is approximately:

$$G_{C\_HF} = 20\log_{10}\left(\frac{R_2}{R_1}\frac{R_6+R_7}{R_6}\right) \cong 26\text{dB}. \quad (20)$$

The extra 16dB gain at high-frequency is a result of the input pre-emphasis network.

In the circuit of Figure 18, we implemented the signal-path pre-emphasis with an additional opamp in order to minimize noise, rather than with a series R-C network in parallel with the VCA input resistor

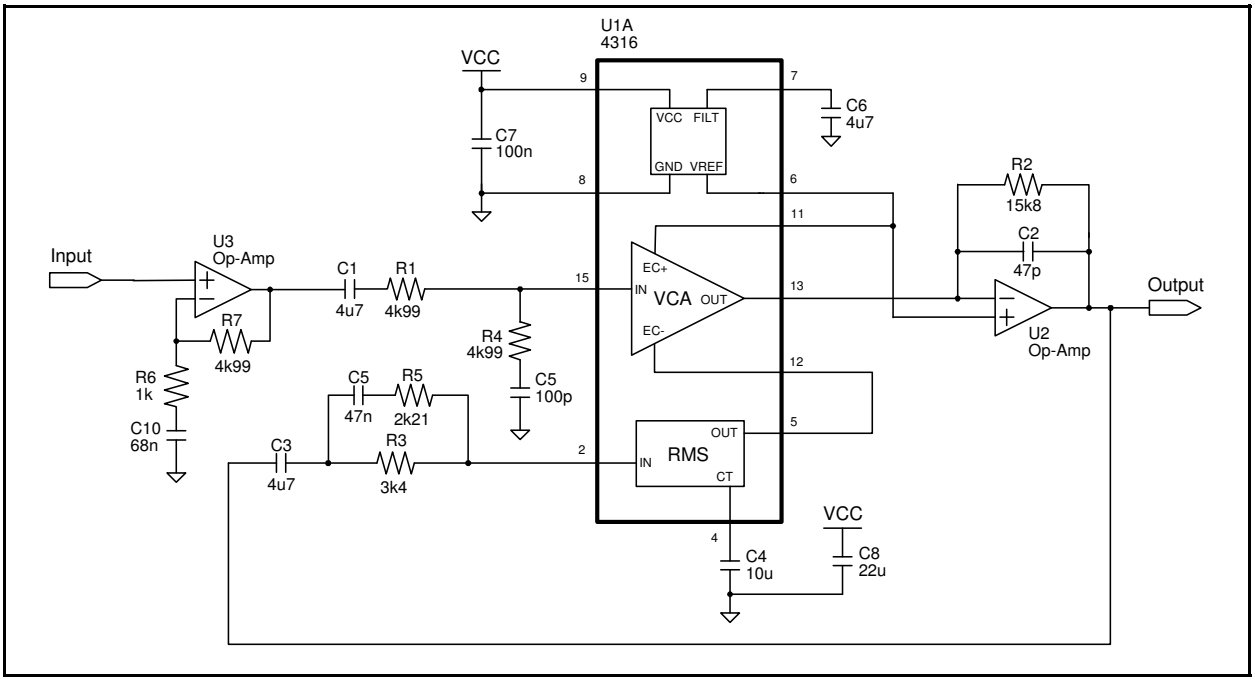

Figure 18. High-performance 2:1 Encoder circuit.

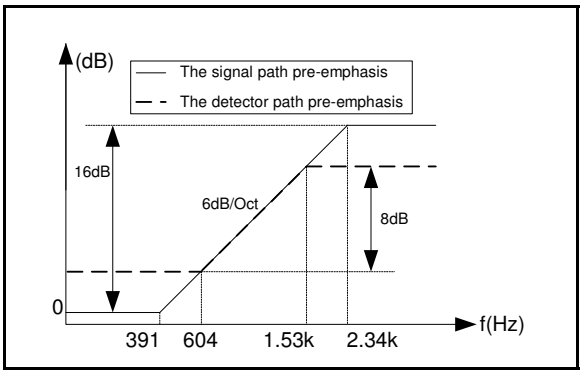

Figure 19. Bode plot of the signal-path and detector-path pre-emphasis of the Fig. 18 Encoder.

R_1. This is because, for gains of unity and above, the 4316 VCA's dominant noise source is its input noise voltage, so reducing the current-to-voltage conversion impedance at the VCA input results in a proportional increase in the output noise. This is undesirable. However, if the pre-emphasis network is placed in a low-noise buffer stage in front of the VCA, there will be less noise at the output of the compressor.

The 16dB high-frequency gain added by the signal-path pre-emphasis increases the compressor's output level at high frequencies. This can cause premature overload in the transmission channel. This undesirable effect is offset by the pre-emphasis in the detection path shown in Figure 18.

With the addition of the pre-emphasis, the RMS detector's reference voltage also becomes frequency dependent as in Equation 21:

$$RMS_{0C} = 20\log_{10}\left(i_{in0} \cdot R_3 \frac{1+sC_5R_5}{1+sC_5(R_3+R_5)}\right). \quad (21)$$

The 2nd term inside the logarithm is the RMS detector's input pre-emphasis network impedance. The RMS input current is proportional to the reciprocal of the impedance. The bode plot for this current (the detector path pre-emphasis) is also drawn in Figure 19. Its corner frequencies, f_3 and f_4, are expressed in Equation 22 and 23, respectively.

$$f_3 = \frac{1}{2\pi(R_3+R_5)C_5} \quad (22)$$

$$f_4 = \frac{1}{2\pi R_5 C_5} \quad (23)$$

For the case in Figure 18, at frequencies substantially under 604 Hz (f_3), the detector's input network's impedance is R_3. Hence, RMS_{0C} in that region is -32.2dBV. At frequencies substantially above 1.53kHz (f_4), the impedance is approximately the parallel combination of R_3 and R_5, *i.e.*, 1.34 kΩ. So RMS_{0C} reduces to -40.3dBV, making the detector more sensitive at high frequencies. Note that the geometric center frequencies for the signal-path and RMS detector pre-emphasis networks are about the same, which is 0.96kHz, *i.e.*, $\sqrt{f_1 f_2} = \sqrt{f_3 f_4}$. The detector pre-emphasis gain is 8dB, about half that of the signal path.

Increasing the detector's sensitivity at high frequencies through pre-emphasis causes it to weight high frequencies more heavily, hence, reducing gain more strongly to high frequencies than to low ones. The right mix of signal-path and detector pre-emphasis avoids high-frequency overload which would otherwise occur.

High-Performance 2:1 Decoder

The decoder shown in Figure 20 matches the encoder of Figure 18. It includes a signal-path

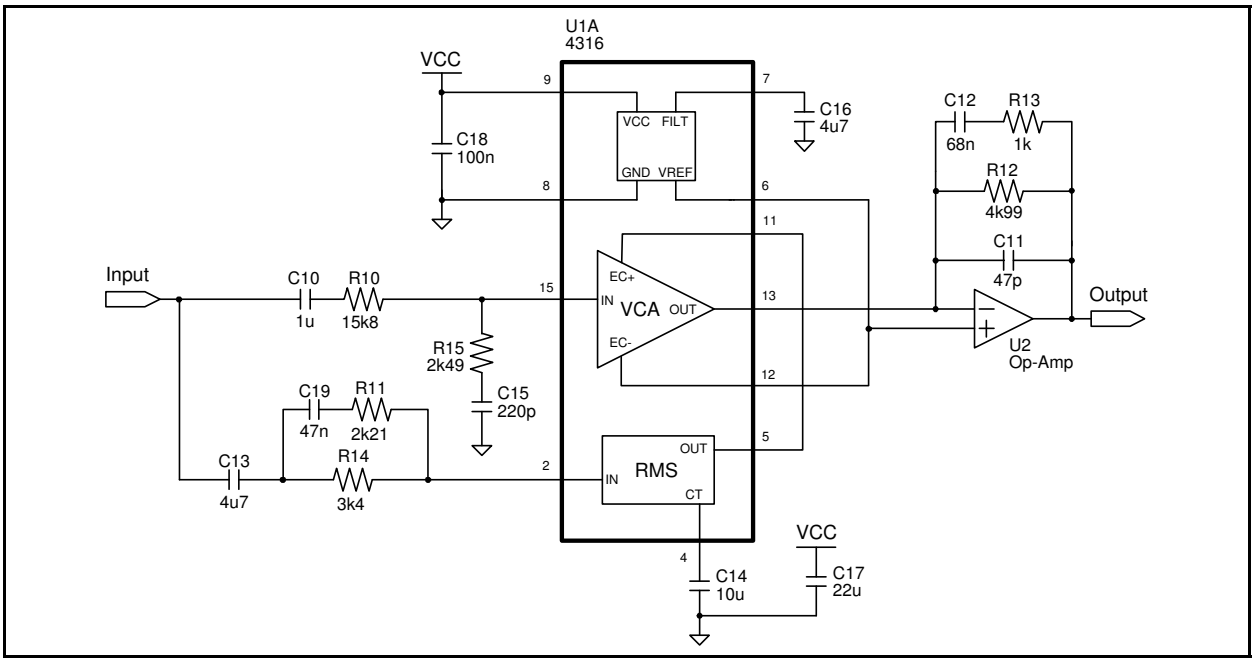

Figure 20. High-performance 2:1 Decoder circuit.

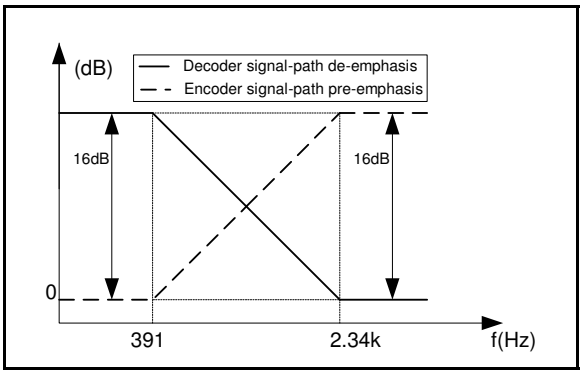

Figure 21. Bode plots of the Fig. 20 Decoder de-emphasis gain and the Fig. 18 Encoder pre-emphasis gain.

de-emphasis network that has inverse frequency response to that of the encoder's signal-path pre-emphasis network as in Figure 21. Equation 8 in the previous section is still applicable. But the signal-path gain G_E becomes frequency dependent and is shown in Equation 24.

$$G_E = 20\log_{10}\left[\frac{1}{R_{10}}\frac{R_{12}(sC_{12}R_{13}+1)}{sC_{12}(R_{12}+R_{13})+1}\right] \quad (24)$$

Encoder In	Encoder VCA Gain	Encoder Out/ Decoder In	i_{in_RMS}	Decoder VCA Gain	Decoder Out
(dBV)	(In dB)	(dBV)	(µA)	(In dB)	(dBV)
0	-21	-11	81.83	21	0
-10	-16	-16	46.02	16	-10
-20	-11	-21	25.88	11	-20
-30	-6	-26	14.55	6	-30
-40	-1	-31	8.18	1	-40
-50	4	-36	4.600	-4	-50
-60	9	-41	2.590	-9	-60
-70	14	-46	1.460	-14	-70
-80	19	-51	0.820	-19	-80
-90	24	-56	0.460	-24	-90
-100	29	-61	0.260	-29	-100

Table 2. High-performance 2:1 compander transfer characteristics (f << 391Hz).

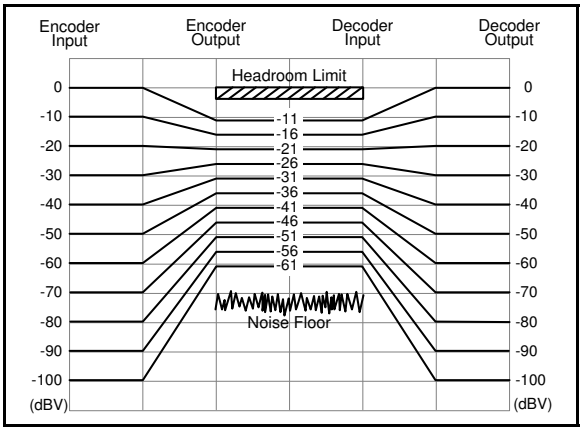

Figure 22. Butterfly diagram of the High-performance 2:1 compander (f << 391Hz).

The same values of R_1 and R_7 in Figure 18 makes it possible to reuse the signal pre-emphasis network as part of the de-emphasis one at the VCA output in Figure 20. The resulting in de-emphasis network ensures that G_E is complementary to the encoder G_C over frequency. Because an identical pre-emphasis network is employed in the decoder detector path, the expander detector reference RMS_{0E} is also frequency dependent and cancels out the RMS_{0C} in the compander system.

Table 2 and Figure 22 show the low-frequency transfer characteristics of the high-performance 2:1 companding system. The encoder VCA gain varies between -21dB and +29dB for an input dynamic range of 100dB. At the same time, the RMS detector current levels i_{in_RMS} varies from 0.26µA to 82µA and $R_{in\_RMS}=R_3=3.4k\Omega$.

The high-frequency transfer characteristics are shown in Table 3 and Figure 23. Because of the detector pre-emphasis, the high frequency signal level at the compressor's output is only 4dB higher than that at the lower frequencies, even with 16dB signal pre-emphasis. The VCA gain range changes to between -33dB and +17dB, and $R_{in\_RMS}=1.34k\Omega$, and i_{in_RMS} shifts up to between 1µA and 319.2µA. All are well within the reach of the 4316.

Encoder In	Encoder VCA Gain	Encoder Out/ Decoder In	i_{in_RMS}	Decoder VCA Gain	Decoder Out
(dBV)	(In dB)	(dBV)	(µA)	(In dB)	(dBV)
0	-33	-7	319.2	33	0
-10	-28	-12	179.5	28	-10
-20	-23	-17	100.9	23	-20
-30	-18	-22	56.76	18	-30
-40	-13	-27	31.92	13	-40
-50	-8	-32	17.95	8	-50
-60	-3	-37	10.09	3	-60
-70	2	-42	5.680	-2	-70
-80	7	-47	3.190	-7	-80
-90	12	-52	1.790	-12	-90
-100	17	-57	1.010	-17	-100

Table 3. High-performance 2:1 compander transfer characteristics (f >> 2.34kHz).

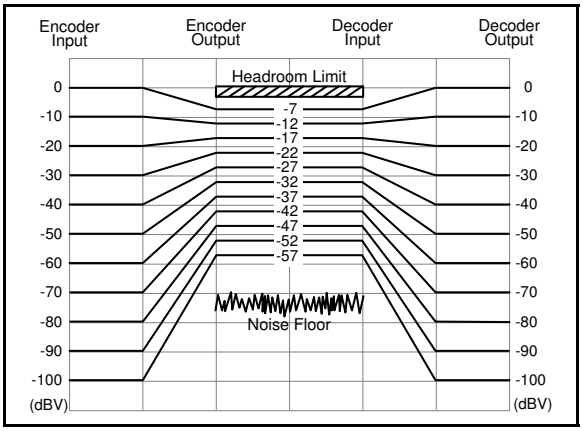

Figure 23. Butterfly diagram of the High-performance 2:1 compander (f >> 1.53kHz).

In this design, we set the maximum encoder output level to -7dBV (or 0.63V_{peak}). This level is well within the voltage capabilities of most 3.3 or 5 V opamps used for U2 in Figure 18 and 20. Additionally, if the designer wishes to limit the voltage swing at the VCA's output to prevent over-modulation in the transmission channel, a pair of back-to-back silicon diodes across R_{12} will accomplish this quite easily, limiting peak swings to about ±0.7V.

Compared to the basic 2:1 compander responses shown in Figure 17, the signal levels at the encoder output are approximately 3 to 7 dB higher over the audio frequency range. This is well predicted by Equation 1. For instance, at low frequencies, the 10dB higher gain and over 3dB lower RMS reference voltage level of the high-performance encoder result in the overall ~3dB higher level at the encoder output. The selection of the gain and RMS reference level is application dependent. It depends on the dynamic range of source signals, transmission channel characteristic and supply level, etc.

In the high-performance compander, any noise in the channel is attenuated at high frequencies by the ~16dB high-frequency attenuation of the decoder signal-path de-emphasis network. This makes a dramatic difference in the perception of the channel noise, and improves masking of the channel noise by the signal.

As a result, we observe about 5.3dB (A-weighted) improvement in the noise floor of the high performance 2:1 compander compared to the basic 2:1 compander. In fact, an even better improvement is expected in reality as the channel noise is not included in the simulation. But, perhaps more importantly, the signal path pre- and de-emphasis combination helps low-frequency signals better mask the acqua noise of a typical FM transmission channel. And, the pre-emphasis in the detector minimizes transient overload that might result from the signal-path pre-emphasis.

3:1 Compander

The flexible configuration of THAT Corporation's Analog Engine® ICs allows compression and expansion ratios of other than 2:1. This feature can be particularly advantageous in situations where RF bandwidth and power are at a premium. The circuits in Figure 24 and 25 demonstrate a 3:1 companding system with pre- and de-emphasis in the signal path, and pre-emphasis in the detector path.

The topology of this system is similar to the previous examples. The transfer functions for a compander system in Equations 1, 8, and 14 still apply, but because of amplifier U3 (with a gain of 2) between the RMS detector output and the VCA control ports (in both the encoder and decoder), the gain factor $K_C=K_E=2$, and thus CR=ER=3:1.

We chose an inverting topology for the gain stage U3 is to minimize the loading to the on-chip VREF generator. Because this inverts the polarity of the control voltage, we swapped the VCA control ports (using E_{C+} for the encoder and E_{C-} for the decoder).

For the 3:1 compressor, pre-emphasis in the detector is even more important than for a 2:1 system. This is because the higher compression ratio leads to more aggressive VCA gain variations as input signal levels change. Making the detector more sensitive at high frequencies helps mitigate potential transient overload at the compressor output. when the input goes from very low to very high quickly. Besides that, the detector pre-emphasis also results in a flatter swept sine-wave response from input to output of the compressor.

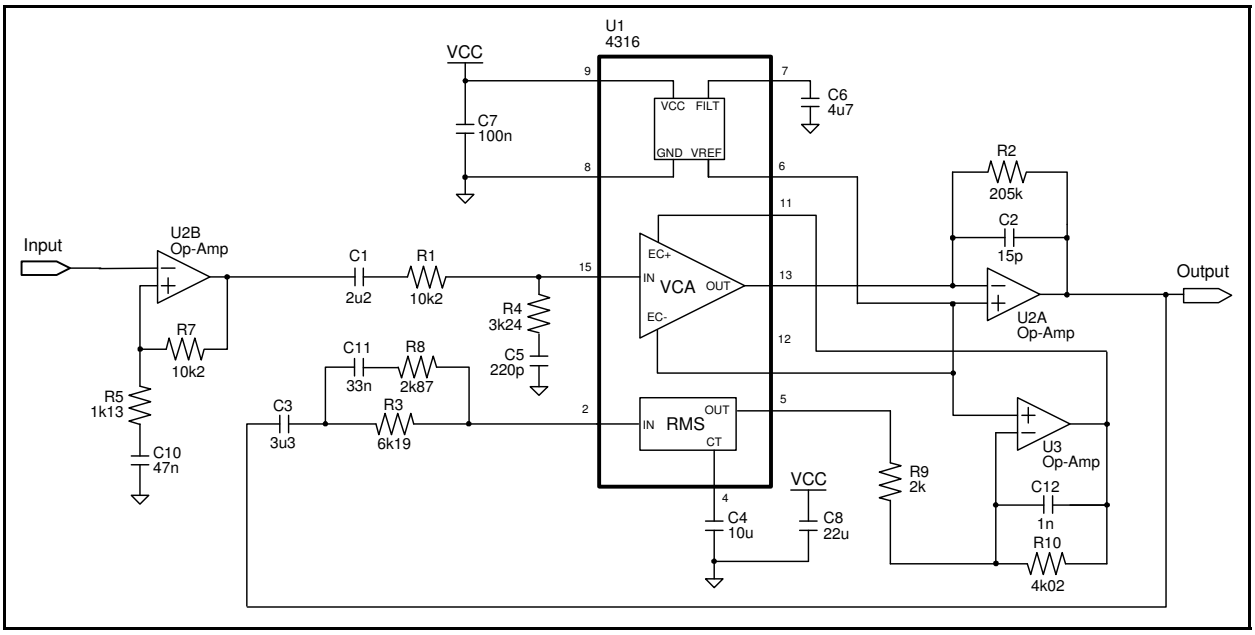

Figure 24. 3:1 Encoder circuit.

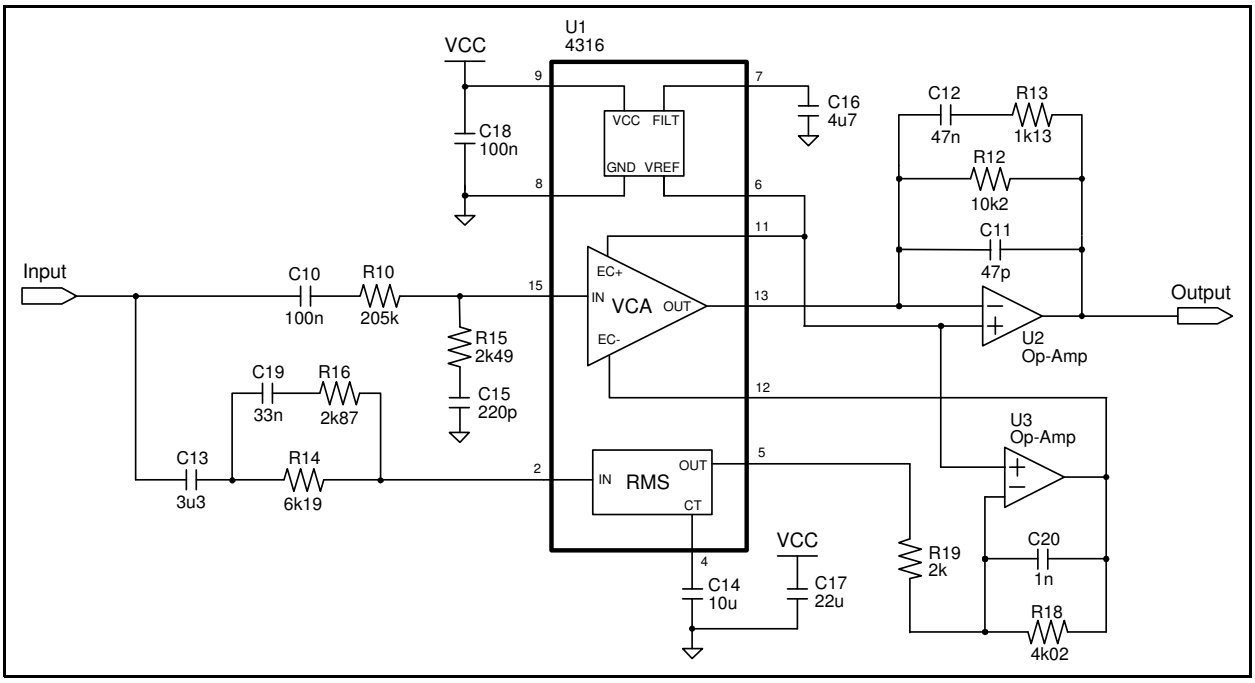

Figure 25. 3:1 Decoder circuit.

The transfer functions for the frequency-dependent G_C and G_E in Equations 16 and 20 still apply. In Figure 24, the signal path pre-emphasis starts at f_1=299Hz and flattens at f_2=3kHz. The encoder low-frequency signal gain is 26dB. The pre-emphasis boosts G_C by 20dB. Hence, at f >> f_2, the signal gain G_C increases to 46dB.

Equation 21 for the frequency-dependent detector reference voltage also applies here. The RMS detector pre-emphasis starts at 532Hz and ends at 1.68kHz. And the high frequency boost is about 10 dB, half that of the signal path pre-emphasis. The center frequencies in the signal and detector paths are also set to be the same, ~0.95kHz. The identical detector pre-emphasis network is employed in the complimentary 3:1 decoder circuit as in Figure 25.

Table 4 and 5 list the transfer characteristics of the 3:1 compander at low and high frequencies, respectively. The amount of pre-emphasis chosen for the RMS detector path makes the encoder output levels stay the same over frequency. So the over-frequency compander level transfer is represented in one single butterfly plot, Figure 26.

As in the previous two compander examples, for a 100dB input dynamic range, the channel dynamic range requirement here is also scaled by CR, but here is equal to 33dB: one-third of the input signal dynamic range. Since the encoder compresses the input signal more than that in the 2:1 systems, the VCA gain changes over a wider range, *i.e.*, -19dB to +47dB at low frequencies and -35dB to +32dB at high frequencies, which is two-thirds of the input dynamic range.

The RMS detectors input current varies over a narrower range, which follows the channel dynamic range. At frequencies well below 532 Hz, R_{in_RMS}=6.19kΩ and i_{in_RMS} varies from 1.19µA to 55.1µA; for frequencies above 1.68kHz, R_{in_RMS} decreases to 1.96kΩ, hence i_{in_RMS} shifts up accordingly to between 3.75µA and 174.1µA. The detector-path pre-emphasis yields a flat overall frequency response at the encoder output, so the encoder outputs at low and high frequencies are the same.

Finally, we set the decoder's maximum output level to -9dB ($0.5V_{peak}$) to make it easy to use a diode clipper at the VCA output for over-modulation protection.

Other Dynamics Processor Configurations

The same distinguishing features that make the 4316 so applicable to companding noise reduction systems also qualify it for dynamics processors of many other types. Because of its low-voltage supply rails and micro power demand, the 4316 is especially applicable to dynamic processors that run from battery power. The 4316 is versatile enough to be used as the heart of a compressor, expander, noise gate, AGC, de-esser, frequency-sensitive compressor, and many other dynamics processors. It is beyond the scope of this data sheet to provide specific advice about these many functional classes. But, we refer interested readers to THAT's many Design Notes covering compressors, limiters, and other dynamic processors. With minor modifications, most of the teachings of those notes apply directly to the 4316.

Encoder In	Encoder VCA Gain	Encoder Out/ Decoder In	i_{in_RMS}	Decoder VCA Gain	Decoder Out
(dBV)	(In dB)	(dBV)	(uA)	(In dB)	(dBV)
0	-19	-9	55.08	19	0
-10	-13	-13	37.53	13	-10
-20	-6	-16	25.57	6	-20
-30	1	-19	17.42	-1	-30
-40	7	-23	11.870	-7	-40
-50	14	-26	8.080	-14	-50
-60	21	-29	5.510	-21	-60
-70	27	-33	3.750	-27	-70
-80	34	-36	2.560	-34	-80
-90	41	-39	1.740	-41	-90
-100	47	-43	1.190	-47	-100

Table 4. 3:1 compander transfer characteristics at f << 299Hz.

Encoder In	Encoder VCA Gain	Encoder Out/ Decoder In	i_{in_RMS}	Decoder VCA Gain	Decoder Out
(dBV)	(In dB)	(dBV)	(uA)	(In dB)	(dBV)
0	-35	-9	174.07	35	0
-10	-28	-13	118.59	28	-10
-20	-22	-16	80.80	22	-20
-30	-15	-19	55.05	15	-30
-40	-8	-23	37.50	8	-40
-50	-2	-26	25.55	2	-50
-60	5	-29	17.410	-5	-60
-70	12	-33	11.860	-12	-70
-80	18	-36	8.080	-18	-80
-90	25	-39	5.500	-25	-90
-100	32	-43	3.750	-32	-100

Table 5. 3:1 compander transfer characteristics at f >> 3kHz.

Please check with THAT's applications engineering department to see if your application has been covered yet, and for personalized assistance with specific designs.

Where to go from here

The design of compander systems and dynamics processors is a very intricate art: witness the proliferation of companding systems, and the many different dynamics processors available in the market today. In the applications section of this data sheet, we offer a few examples of companders as a starting point only. THAT Corporation's applications engineering department is ready to assist customers with suggestions for tailoring and extending these basic circuits to meet specific needs.

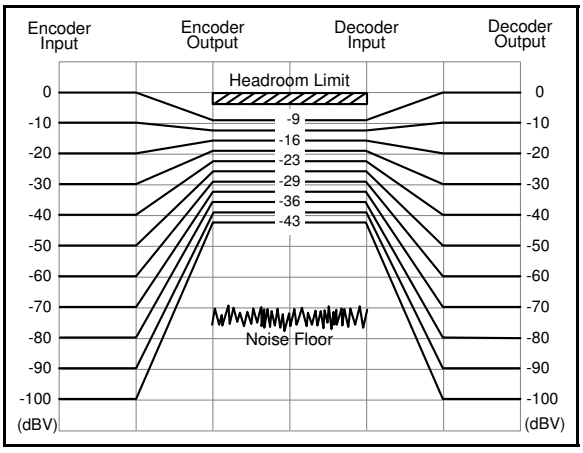

Figure 26. Butterfly diagram of the 3:1 compander.

Package Characteristics

Parameter	Symbol	Conditions	Typ	Units
Surface Mount Package				
Type		See below for pinout and dimensions	16 pin QSOP	
Thermal Resistance	θ_{JA}	QSOP package soldered to board	150	ºC/W
Soldering Reflow Profile			JEDEC JESD22-A113-D (260 ºC)	

Package Information

The THAT 4316 pins are listed in Table 6. The part is available in a 16-pin QSOP package as shown in Figure 27.

Pin Name	Pin Number
No Internal Connection	1
RMS IN	2
No Internal Connection	3
CT	4
RMS OUT	5
V_{REF}	6
FILTER	7
GND	8
V_{CC}	9
No Internal Connection	10
EC+	11
EC-	12
VCA OUT	13
No Internal Connection	14
VCA IN	15
No Internal Connection	16

Table 6. THAT 4316 pin assignments.

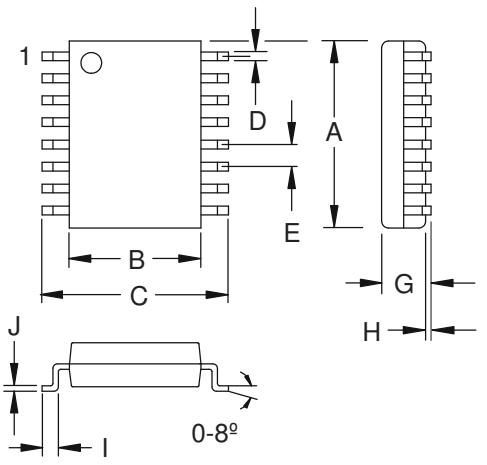

ITEM	MILLIMETERS	INCHES
A	4.80 - 4.98	0.189 - 0.196
B	3.81 - 3.99	0.150 - 0.157
C	5.79 - 6.20	0.228 - 0.244
D	0.20 - 0.30	0.008 - 0.012
E	0.635 BSC	0.025 BSC
G	1.35 - 1.75	0.0532 - 0.0688
H	0.10 - 0.25	0.004 - 0.010
I	0.40 - 1.27	0.016 - 0.050
J	0.19 - 0.25	0.0075 - 0.0098

Figure 27. Surface mount package QSOP-16.

Revision History

Revision	Date	Changes	Page
00	10/12/12	Initial release	—

THAT Corporation; 45 Sumner Street; Milford, MA 01757-1656; USA
Tel: +1 508 478 9200; Fax: +1 508 478 0990; Email: info@thatcorp.com; Web: www.thatcorp.com

Notes

THAT Corporation; 45 Sumner Street; Milford, MA 01757-1656; USA
Tel: +1 508 478 9200; Fax: +1 508 478 0990; Email: info@thatcorp.com; Web: www.thatcorp.com